Dental Materials Journal 2014; 33(6): 805–810

Hydration kinetics, ion-release and antimicrobial properties of white Portland cement blended with zirconium oxide nanoparticles

Qiu LI[1,2] and Nichola J. COLEMAN[3]

[1] *State Key Laboratory of Silicate Materials for Architectures, Wuhan University of Technology, Wuhan 430070, China*
[2] *Green Building Materials Manufacturing and Engineering Research Centre of MOE, Wuhan University of Technology, Wuhan 430070, China*
[3] *School of Science, University of Greenwich, Chatham Maritime, Kent, ME4 4TB, UK*
Corresponding author, Nichola J. COLEMAN; E-mail: nj_coleman@yahoo.co.uk

This study examines the impact of 20 wt% zirconium oxide nanoparticles on the early hydration kinetics of white Portland cement by isothermal conduction calorimetry and transmission electron microscopy. The findings confirm that the nano-ZrO_2 particles do not directly participate in the chemical reactions during cement hydration; although, they do divert the normal hydration processes and accelerate the initial setting reactions. The rate of heat evolution and the extent of the exotherm associated with these reactions are reduced in the presence of nano-ZrO_2. The incorporation of nano-ZrO_2 into the cement also decreases the solubility of the silicate phases but does not compromise its capacity to release hydroxide ions. There was no observed difference in the antimicrobial activity of the nano-ZrO_2-blended and unblended cement pastes against *S. aureus* and *E. coli*; however, a modest reduction in this property was noted against *P. aeruginosa* for the blended cement.

Keywords: Cement hydration, Radiopacifier, Zirconium oxide, Nanoparticles, Isothermal conduction calorimetry

INTRODUCTION

Mineral trioxide aggregate (MTA) is a clinical product comprising an 80:20 wt% mixture of Portland cement and bismuth oxide (Bi_2O_3), a radiopacifier, which has been used in endodontics since the mid-1990s[1,2]. 'Tooth-colored' ProRoot MTA is formulated with white Portland cement (WPC) and is presented as a powder which is mixed manually with supplied sterile water.

The principal components of WPC are: 'alite' (Ca_3SiO_5); 'belite' (β-Ca_2SiO_4); 'aluminate' ($Ca_3Al_2O_6$); and 'ferrite' ($Ca_2(Al/Fe)O_5$) which contain substituted main group and transition metal ions[3,4]. Up to 5% of gypsum ($CaSO_4.2H_2O$) is also ground into the anhydrous cement to moderate the setting of the aluminate phase. During grinding a proportion of the gypsum is commonly dehydrated to form calcium sulphate hemihydrate ($CaSO_4.0.5H_2O$). On mixing with water, complex chemical reactions give rise to hydrated phases that form an adhesive matrix which hardens and sets. During hydration, alite and belite give rise to a non-stoicheiometric poorly crystalline calcium silicate hydrate (C-S-H) gel phase, of approximate formula $Ca_3Si_2O_7.3H_2O$, and portlandite ($Ca(OH)_2$). The initial reactions of the aluminate and ferrite phases with gypsum and water yield lath-like crystals of ettringite ($6CaO.Al_2O_3.3SO_3.32H_2O$) and its Fe-substituted analogue, which are dispersed throughout the matrix[3,4].

Bismuth oxide is essentially inert with respect to the hydration chemistry of WPC, in that it is not incorporated into the product phases; however, it is reported to retard hydration, prolong setting time, increase porosity, and reduce durability[2,5,6]. Bismuth oxide is also reported to exhibit toxicity towards human dental pulp and periodontal ligament cells[7,8]. Alternative radiopacifying agents with superior physicochemical properties and biocompatibility are currently under consideration. Zirconium oxide, ZrO_2, is among these candidate radiopacifiers as it is bioinert, biocompatible and is currently used in the reconstruction of skeletal and dental tissues[8-11]. In particular, zirconium oxide nanoparticles, nano-ZrO_2, have recently been shown to accelerate the hydration of WPC and to improve its biocompatibility with respect to human osteosarcoma cells *in vitro*[12].

The principal aims of this study were to investigate the impact of 20 wt% of nano-ZrO_2 on the kinetics of WPC hydration by isothermal conduction calorimetry and to evaluate the antimicrobial activity and ion-release properties of the blended cement paste. The microbial resistance of the nano-ZrO_2-blended and unblended pastes against *Staphylococcus aureus*, *Escherichia coli* and *Pseudomonas aeruginosa* were determined *via* the Kirby-Baur inhibition zone method, and their ion-release behaviour was monitored during immersion in simulated body fluid. The null hypothesis that the incorporation of 20 wt% of nano-ZrO_2 would not affect the antimicrobial properties of the cement was tested at p=0.05 *via* a two-tailed t-test.

MATERIALS AND METHODS

Materials, preparation and characterisation

The WPC used in this study was supplied by Lafarge and is commercially available as 'Snowcrete'. Its major oxide and phase compositions were provided by the manufacturer and are listed in Table 1. Zirconium oxide nanoparticles, in the 50–75 nm diameter range, were purchased from Sigma Aldrich and used as received. Cement paste specimens (labelled 'WPC') were prepared

Received Jun 11, 2014: Accepted Jul 22, 2014
doi:10.4012/dmj.2014-174 JOI JST.JSTAGE/dmj/2014-174

Table 1 Composition of white Portland cement

Major oxide components		Major crystalline phases	
Formula	Mass (%)	Formula	Mass (%)
CaO	69.2	Ca_3SiO_5	65
SiO_2	25.0	Ca_2SiO_4	22
Al_2O_3	1.76	$Ca_3Al_2O_6$	4.1
SO_3	2.00	$Ca_2(Al/Fe)O_5$	1.0

in triplicate by manually mixing 10 g of cement powder with 3.75 g of distilled water (*i.e.* at a water:cement ratio of 0.375 by mass) for 5 min. Nano-ZrO_2-blended samples (*viz.* 'WPC-Zr') were prepared similarly with partial replacement of the cement powder with 20 wt% zirconium oxide nanoparticles at a water:cement ratio of 0.375.

Isothermal conduction calorimetry

The rates of heat evolution during hydration of the WPC and WPC-Zr cement samples were measured by isothermal conduction calorimetry using a Thermometric 2277 TAM calorimeter at 37.5°C. In each case, ~0.1 g of accurately weighed cement paste was placed in the calorimeter immediately after mixing. Power (*i.e.* the rate of heat evolution) data was collected every second for 40 h. The rate of heat evolution *per* unit kilogram of cement powder was then calculated by dividing the power data by the original mass of white Portland cement in the sample paste.

Transmission electron microscopy (TEM)

TEM images of WPC and WPC-Zr, after curing for 3 h at 37°C in sealed polypropylene containers, were obtained by dispersing the ground samples in methanol prior to deposition onto a carbon film grid. Bright field images were obtained using a JEOL JEM200CX microscope fitted with a Gata Orius SC200 digital camera.

Ion-release of WPC and WPC-Zr in SBF

WPC and WPC-Zr cement paste discs, 1.0 mm thick and measuring 10 mm in diameter, were cast into polypropylene moulds and cured at 37°C for 6 h. Simulated body fluid (SBF) was prepared in accordance with the method described by Kokubo and Takadama[13] and stored at 4°C for no longer than 3 days prior to use. One disc of either WPC or WPC-Zr was contacted with 40 cm^3 of SBF in hermetically sealed polypropylene containers at 37°C for time intervals of 3, 24, 48, 72, and 168 h. Each analysis was carried out in triplicate. The pH values of the supernatant liquors were measured using a Corning 140 pH meter and solution concentrations of Si, Ca, P, Al and Zr species were monitored by ICP using a TJA Iris simultaneous ICP-OES and matrix-matched multi-element standards. The solid specimens were recovered from solution, rinsed with distilled water and dried in air at 37°C for 24 h prior to analysis by Fourier transform infrared spectroscopy (FTIR) using a Perkin Elmer Paragon 1000 FTIR spectrophotometer. Spectra were recorded between 4,000 and 500 cm^{-1}. Cement samples after immersion in SBF for 168 h are denoted as WPC-SBF and WPC-Zr-SBF.

Antibacterial properties of WPC and WPC-Zr

The antimicrobial activities of WPC and WPC-Zr cement pastes were evaluated using the semi-quantitative Kirby-Bauer agar diffusion inhibition zone method against Gram-positive *Staphylococcus aureus* NCIMB 9518, Gram-negative *Escherichia coli* NCIMB 9132 and Gram-negative *Pseudomonas aeruginosa* NCIMB 8628. In each case, 100 cm^3 of Nutrient Broth (Oxoid) was inoculated with 0.1 cm^3 of an overnight culture of the bacterium. The cultures were then incubated for 24 h, with shaking, at 37°C. 0.2 cm^3 of each resulting culture were spread on 8 nutrient agar plates for each cement type. WPC and WPC-Zr cement paste discs, 1.0 mm thick and measuring 10 mm in diameter, were cured at 37°C for 6 h. One disc was placed in the centre of each plate, the plates were incubated at 37°C for 24 h and then examined for clear zones. The inhibition zone data were subjected to a two-tailed *t*-test at (n-2) degrees of freedom and the null hypothesis was tested at p=0.05.

RESULTS

Isothermal conduction calorimetry

The rates of heat evolution *per* kilogram of cement powder for samples WPC and WPC-Zr are plotted in Fig. 1. It should be noted that the initial rapid heat evolution of WPC, arising largely from the wetting process, precipitation of early hydrates and the hydration of free lime and calcium sulphate hemihydrate, which takes place within the first few minutes of mixing is absent from these data, as the calorimeter requires 20 min to equilibrate[14,15]. The strongly exothermic signal at 3 h for sample WPC generates a maximum power of 24.8 W kg^{-1} and is largely attributed to ettringite formation. The subsequent 'acceleratory period' is characterized by rapid hydration which is determined by the rate of formation of the C-S-H gel product phase[14,15]. The maximum rate of heat evolution during the acceleratory period for WPC is 5.20 W kg^{-1} which occurs 5 h after mixing. The deceleratory stage which follows marks a decline in hydration rate as the reactions become diffusion controlled.

The rate of heat evolution profile for sample WPC-Zr differs considerably from that of the unblended cement paste (Fig. 1). This curve exhibits a doublet signal with maxima of 5.90 W kg^{-1} and 7.65 W kg^{-1} at 45 min and 1 h, respectively. A dormant phase is then noted until 4 h into the hydration process with the advent of the acceleratory period which reaches a maximum rate of heat evolution of 4.85 W kg^{-1} at 9 h. The total heats of hydration of samples WPC and WPC-Zr *per* kilogram of cement at 40 h are 260 kJ kg^{-1} and 290 kJ kg^{-1}, respectively, and are obtained from the areas under the power curves.

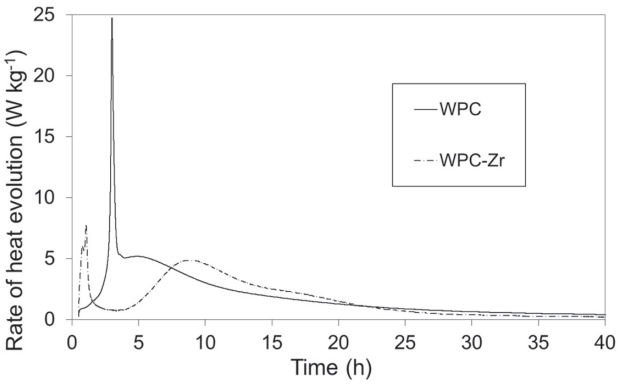

Fig. 1 The rates of heat evolution of WPC and WPC-Zr during hydration at 37°C.

Transmission electron microscopy

TEM bright field images of WPC (Fig. 2(a)) and WPC-Zr (Fig. 2(b)) after curing for 3 h indicate that both samples contain lath-like crystals of ettringite of varying sizes and a C-S-H gel phase. The C-S-H gel phase is principally found to be precipitated onto the surfaces of the ZrO_2 nanoparticles (Fig. 2(b)), and the presence of the ZrO_2 nanoparticles reduces the size of the ettringite crystals. TEM analysis also confirmed that the nano-ZrO_2 particles remain intact during the hydration reactions and that zirconium is not chemically incorporated into the C-S-H gel and ettringite product phases.

Ion-release of WPC and WPC-Zr in SBF

The FTIR spectra of WPC and WPC-Zr are shown in Fig. 3. The combination band at 980 cm^{-1} arises from Si-O stretching modes in C-S-H gel with contributions at 870 and 1,120 cm^{-1} from carbonate and sulphate groups, respectively[16]. The signal at 1,490 cm^{-1} also arises from carbonate species, and the broad bands at 1,660 and 3,470 cm^{-1} are attributed to O-H vibrations of free water in the pores of the cement matrix, bound water, and hydroxyl groups of the hydration products. Crystalline portlandite gives rise to the sharp O-H stretching band at 3,670 cm^{-1} in both cements and the bands at 580 and 745 cm^{-1} in the spectrum of WPC-Zr arise from Zr-O vibrational modes[17].

The FTIR spectra of WPC and WPC-Zr following immersion in SBF for 168 h are also shown in Fig. 3. The dissolution of portlandite from both cements in contact with SBF is denoted by the absence of the sharp signal at 3,670 cm^{-1}. The deposition of hydroxyapatite on the surfaces of both cements is indicated by the broadening of the Si-O stretching signals and a shift in these maxima from 980 cm^{-1} to 1,050 cm^{-1} owing to the superposition of the phosphate P-O stretching modes at 960, 1,060, and 1,100 cm^{-1} over this band[18]. The characteristic doublet at 570 and 605 cm^{-1} which arises from P-O bending vibrations in crystalline hydroxyapatite is clearly visible in the spectrum of WPC-SBF; however, this signal is obscured by Zr-O vibrations in the spectrum of WPC-

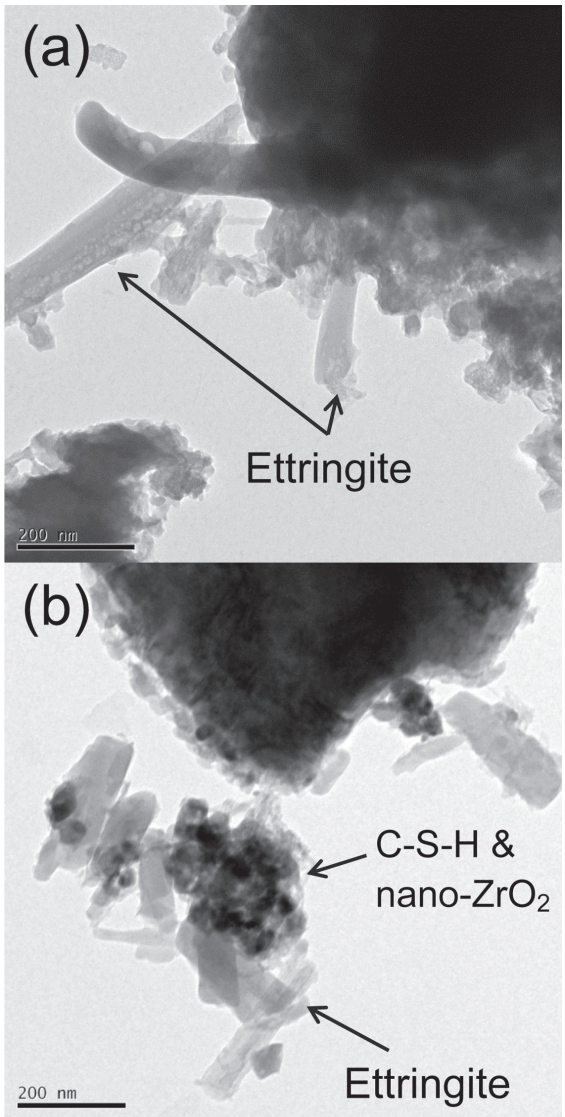

Fig. 2 TEM micrographs of (a) WPC and (b) WPC-Zr.

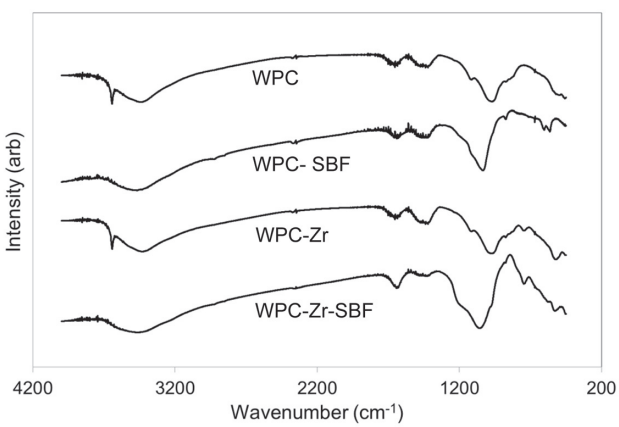

Fig. 3 FTIR spectra of WPC, WPC-SBF, WPC-Zr and WPC-Zr-SBF.

Zr-SBF.

The concentration profiles of Ca, Si, and P species in the supernatant SBF solutions as functions of time are presented in Fig. 4, and the corresponding pH data are given in Fig. 5. The ionic concentration and pH profiles are consistent with the FTIR data and indicate the dissolution of portlandite and the concurrent removal of phosphate ions from SBF during the precipitation of an apatite layer. These data show that the rate and extent of calcium dissolution from WPC-Zr are lower than those of its unblended counterpart, and reflect the lower cement-content of this material. Conversely, the concomitant rises in pH of the SBF solutions from 7.4 to 8.20 (for WPC) and 8.18 (for WPC-Zr) after 168 h were not significantly different despite the 20% reduction in cement-content of WPC-Zr.

The removal of phosphate ions from SBF solution is initially less rapid for the ZrO_2-blended cement; however, after 24 h both supernatant solutions are essentially depleted of phosphate ions (Fig. 4). The dissolution of silicate species from both cements reaches a maximum at 3 h and falls to below 0.5 ppm after 48 h, although the maximum soluble silicate concentration of WPC (45 ppm) is five times higher than that of WPC-Zr (7 ppm). Throughout the investigation, the concentrations of Al and Zr species remained below the limits of detection (0.01 ppm).

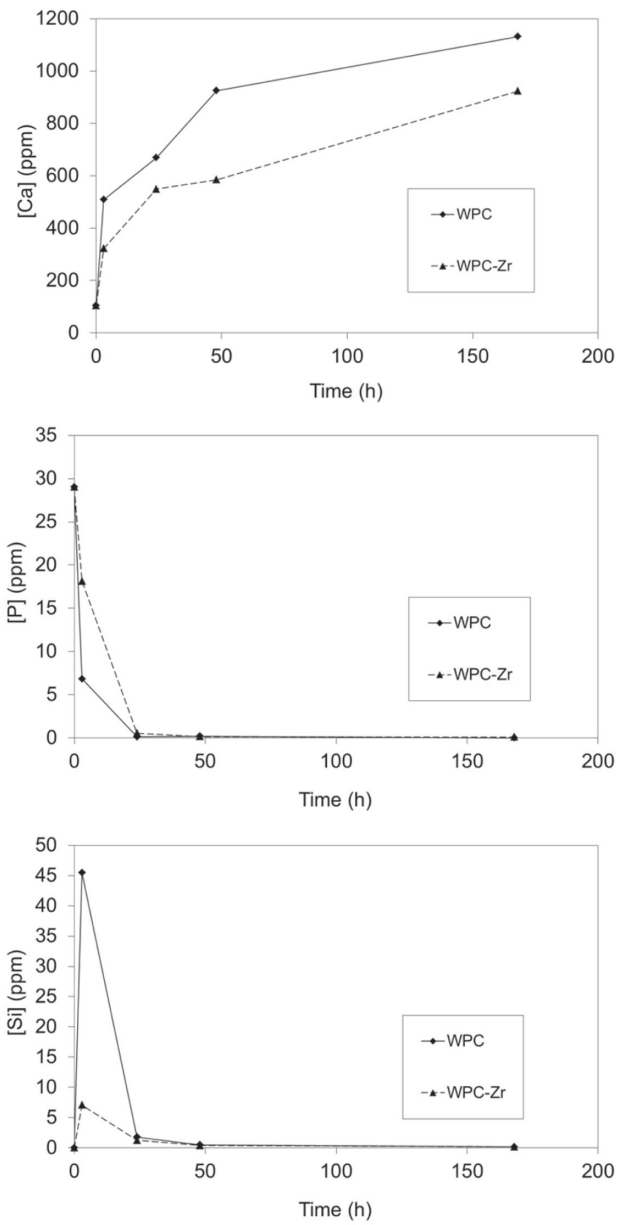

Fig. 4 Concentration profiles for Ca, P and Si in the supernatant SBF solutions in contact with WPC and WPC-Zr.

Antibacterial properties of WPC and WPC-Zr

The inhibition zone data for WPC and WPC-Zr cement pastes in contact with *S. aureus*, *E. coli* and *P. aeruginosa* are listed in Table 2. Clear zones around each of the cement paste discs were noted in all cases indicating that WPC and WPC-Zr are intrinsically antimicrobial against all bacterial strains. There was found to be no significant difference between the size of the inhibition zones around the two cement pastes in contact with *S. aureus* (p=0.39) and *E. coli* (p=0.41); however, a relative

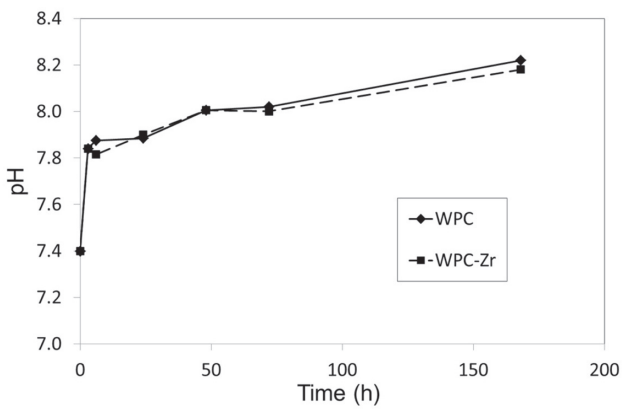

Fig. 5 pH profiles for supernatant SBF solutions in contact with WPC and WPC-Zr.

Table 2 Zone of inhibition data for WPC and WPC-Zr pastes

Bacterium	WPC	WPC-Zr
S. aureus		
Zone of inhibition (mm)	17.6±0.8	17.8±1.0
E. coli		
Zone of inhibition (mm)	14.1±0.9	14.2±1.0
P. aeruginosa		
Zone of inhibition (mm)	17.0±1.3	14.6±0.5

reduction in antimicrobial activity against *P. aeruginosa* was observed for sample WPC-Zr ($p<0.001$).

DISCUSSION

Recent research has shown that the presence of 20 wt% nano-ZrO_2 accelerates the hydration processes of Portland cement and alters the microstructure of the material which improves its biocompatibility with respect to human osteosarcoma cells[12]. In this current study, isothermal calorimetry has confirmed that the incorporation of ZrO_2 nanoparticles diverts the normal hydration chemistry and accelerates the initial setting reactions during which ettringite is produced. The maximum rate of heat evolution during these reactions is considerably lower for the nano-ZrO_2-blended cement and the size of the ettringite crystals is decreased. The reduced exotherm may be an advantage in clinical applications where high rates of heat evolution and elevated temperatures are undesirable.

The solubility of the components of Portland cement-based endodontic restoratives impacts upon their sealing capacity, mechanical stability, antimicrobial properties, biocompatibility and bioactivity[18-21]. For example, soluble calcium and silicate species are acknowledged to stimulate bone tissue regeneration[18,19]. The release of hydroxide ions is associated with antimicrobial activity and also the ability to induce bone mineralisation[11,20,21]. The reaction between released calcium ions and physiological carbonate ions forms insoluble calcite which precipitates in the cracks, pores, voids and margins of the cement and is conjectured to improve the sealing ability of the material[20]. However, it should be noted that, extensive dissolution of the cement phases will undoubtedly lead to the loss of integrity of the material and subsequent mechanical failure.

The ion-release evaluation in this study has shown that the dissolution of both cements is incongruent and that, in general, incorporation of nano-ZrO_2 reduces the solubility of the silicate phases without compromising the cement's ability to release calcium and hydroxide ions. This finding confirms those of Guerreiro-Tanomaru *et al.*[11,21], who report little difference in pH values in distilled water for pure Portland cements and those blended with 30 wt% ZrO_2 micro- and nanoparticles.

Hydroxyapatite was formed on both cements on immersion in SBF, which confirms their *in vitro* bioactivity. However, this process was initially slower for the nano-ZrO_2-blended material.

The antimicrobial activities of WPC and WPC-Zr were tested against *S. aureus*, *E. coli* and *P. aeruginosa*, as these microorganisms have all been isolated from infected root canals[22,23]. The findings indicate that both cements possess intrinsic antibacterial action against all three pathogens, which is principally attributed to their capacity to release hydroxide ions. No difference was observed between the size of the inhibition zones around the two cement paste samples in contact with *S. aureus* and *E. coli*; however, a modest reduction in antimicrobial activity against *P. aeruginosa* was observed for sample WPC-Zr. It is speculated that, in addition to the release of hydroxide ions and associated elevation in pH, the release of silicate species may also contribute to the antimicrobial efficacy of bioactive glasses[24]. Further work would be required to confirm whether the observed reduction in antimicrobial activity of WPC-Zr against *P. aeruginosa* is attributable to the lower concentrations of silicate species released from this material.

Other agar diffusion test studies[21,22] report that 30 wt% addition of nano-ZrO_2 to Portland cement does not compromise its antimicrobial activity against *P. aeruginosa*. Caution must be applied when comparing data between various reported inhibition zone studies, as the outcome of these tests is influenced, not only by the intrinsic properties of the material, but also by other factors such as inoculum density, culture medium, incubation time and agar composition.

In summary, the findings of this study contribute to the burgeoning body of research which suggests that ZrO_2 nanoparticles may be suitable for use as a radiopacifying agent in Portland cement-based materials. However, further research is required to understand how the observed changes in hydration kinetics and cement microstructure will influence the sealing ability and durability of these materials in endodontic applications.

CONCLUSIONS

This study investigates the impact of 20 wt% zirconium oxide nanoparticles on the early hydration kinetics of white Portland cement by isothermal conduction calorimetry and transmission electron microscopy. The nano-ZrO_2 particles do not directly participate in the chemical reactions during cement hydration; although they do accelerate the initial setting and reduce the rate of heat evolution. The incorporation of nano-ZrO_2 particles reduces the solubility of the silicate phases but does not compromise the release of hydroxide ions. There was no observed difference in the antimicrobial activities of the unblended and nano-ZrO_2-blended cement pastes against *S. aureus* and *E. coli*; however, a modest reduction in this property was noted for the blended cement against *P. aeruginosa*.

The accelerated hydration reactions, reduction in the rate of heat evolution and decreased solubility of the silicate phases are potential advantages for nano-ZrO_2-blended Portland cements in endodontic applications.

REFERENCES

1) Roberts HW, Toth JM, Berzins DW, Charlton DG. Mineral trioxide aggregate material use in endodontic treatment: a review of the literature. Dent Mater 2008; 24: 149-164.
2) Darvell BW, Wu RCT. "MTA"-An hydraulic silicate cement: review update and setting reaction. Dent Mater 2011; 27: 407-422.
3) Taylor HFW. Cement Chemistry. 1st ed. London: Academic Press; 1990.
4) Pöllmann H. In: Bensted J, Barnes P, editors. Structure and performance of cements. 1st ed. London: Spon Press; 2002. p. 25-56.
5) Coomaraswamy KS, Lumley PJ, Hofmann MP. Effect

of bismuth oxide radioopacifier content on the material properties of an endodontic Portland cement-based (MTA-like) system. J Endod 2007; 33: 295-298.
6) Li Q, Coleman NJ. Early hydration of white Portland cement in the presence of bismuth oxide. Adv Appl Ceram 2013; 112: 207-212.
7) Min KS, Chang HS, Bae JM, Park SH, Hong CU, Kim EC. The induction of heme oxygenase-1 modulates bismuth oxide-induced cytotoxicity in human dental pulp cells. J Endod 2007; 33: 1342-1346.
8) Kim EC, Lee BC, Chang HS, Lee W, Hong CU, Min KS. Evaluation of the radiopacity and cytotoxicity of Portland cements containing bismuth oxide. Oral Surg Oral Med Oral Pathol Oral Radiol Endod 2008; 105: 54-57.
9) Coleman NJ, Li Q. The impact of zirconium oxide radiopacifier on the early hydration behaviour of white Portland cement. Mater Sci Eng C 2013; 33: 427-433.
10) Duarte MAH, de Oliveira El Kadre GD, Vivan RR, Guerreiro-Tanomaru JM, Tanomaru-Filho M, de Moraes IG. Radiopacity of Portland cement associated with different radiopacifying agents. J Endod 2009; 35: 737-740.
11) Guerreiro-Tanomaru JM, Storto I, da Silva GF, Bosso R, Costa BC, Bernardi MIB, Tanomaru-Filho M. Radiopacity, pH and antimicrobial activity of Portland cement associated with micro- and nanoparticles of zirconium oxide and niobium oxide. Dent Mater J 2014; 33: 466-470
12) Li Q, Deacon AD, Coleman NJ. The impact of zirconium oxide nanoparticles on the hydration chemistry and biocompatibility of white Portland cement. Dent Mater J 2013; 32: 808-815.
13) Kokubo T, Takadama H. How useful is SBF in predicting in vivo bone bioactivity? Biomaterials 2006; 27: 2907-2915.
14) Bensted J. Some applications of conduction calorimetry to cement hydration. Adv in Cem Res 1987; 1: 35-44.
15) Mostafa NY, Brown PW. Heat of hydration of high reactive pozzolans in blended cements: isothermal conduction calorimetry. Thermochimica Acta 2005; 435: 162-167.
16) Bensted J, Varma SP. Some applications of infrared and Raman spectroscopy in cement chemistry, Part 3: Hydration of Portland cement and its constituents. Cem Technol 1974; 5: 440-450.
17) Jayakumara S, Ananthapadmanabhan PV, Perumal K, T.K. Thiyagarajan TK, S.C. Mishra SC, Su LT, Tok AIY, Guo J. Characterization of nano-crystalline ZrO_2 synthesized via reactive plasma processing. Mater Sci Eng B 2011; 176: 894-899.
18) Coleman NJ, Awosanya K, Nicholson JW. Aspects of the *in vitro* bioactivity of hydraulic calcium (alumino)silicate cement. J Biomed Mater Res A 2009; 90: 166-174.
19) Xynos ID, Edgar AJ, Buttery LDK, Hench LL, Polak JM. Gene-expression profiling of osteoblasts following treatment with the ionic products of Bioglass 45S5 dissolution. J Biomed Mater Res 2000; 155: 151-157.
20) Han L, Okiji T, Okawa S. Morphological and chemical analysis of different precipitates on mineral trioxide aggregate immersed in different fluids. Dent Mater J 2010; 29: 512-517.
21) Guerreiro-Tanomaru JM, Cornelio AL, Andolfatto C, Salles LP, Tanomaru-Filho M. pH and antimicrobial activity of Portland cement associated with different radiopacifying agents. ISRN Dent 2012; 469019 DOI: 10.5402/2012/469019.
22) Guimarães, NLSdL, Otoch HM, de Andrade LC, Ferreira CM, Rocha MMdNP, Gomes FdA. Microbiological evaluation of infected root canals and their correlation with pain. RSBO 2012; 9: 31-37.
23) Rani A, Chopra A. Isolation and identification of root canal bacteria from symptomatic non-vital tooth with periapical pathosis. Endodontology 2006; 18: 12-17.
24) Zehnder M, Waltimo T, Sener B, Söderling E. Dentin enhances the effectiveness of bioactive glass S53P4 against a strain of *Enterococcus faecalis*. Oral Surg Oral Med Oral Pathol Oral Radiol and Endod 2006; 101: 530-535.